PHILOSOPHICAL TRANSACTIONS OF THE ROYAL SOCIETY A

Phil. Trans. R. Soc. A (2011) **369**, 957–975
doi:10.1098/rsta.2010.0329

Sediment flux and the Anthropocene

By James P. M. Syvitski* and Albert Kettner

CSDMS Integration Facility, INSTAAR, University of Colorado, Boulder, CO 80309-0545, USA

Data and computer simulations are reviewed to help better define the timing and magnitude of human influence on sediment flux—the Anthropocene epoch. Impacts on the Earth surface processes are not spatially or temporally homogeneous. Human influences on this sediment flux have a secondary effect on floodplain and delta-plain functions and sediment dispersal into the coastal ocean. Human impact on sediment production began 3000 years ago but accelerated more widely 1000 years ago. By the sixteenth century, societies were already engineering their environment. Early twentieth century mechanization has led to global signals of increased sediment flux in most large rivers. By the 1950s, this sediment disturbance signal reversed for many rivers owing to the proliferation of dams, and sediment load reduction below pristine conditions is the dominant signal today. A delta subsidence signal began in the 1930s and is now a dominant signal in terms of sea level for many coastal environments, overwhelming even the global warming imprint on sea level. Humans have engineered how most water and sediment are discharged into the coastal ocean. Hyperpycnal flow events have become more common for some rivers, and less common for other rivers. Bottom trawling is now widespread, suggesting that even continental shelves have received a significant but as yet quantified Anthropocene impact. The Anthropocene attains the level of a geological climate event, such as that seen in the transition between the Pleistocene and the Holocene.

Keywords: sediment flux; human impacts; geo-engineering

1. Introduction

The Anthropocene is being considered as a defined geological epoch, wherein the human species has collectively impacted the Earth's surface so as to result in a global signal in the permanent geological record [1,2]. Most Cenozoic epochs reflect stratigraphic 'events' defined in terms of extinctions, or regional tectonics, or bulk changes in the composition of sedimentary rocks. Have humans contributed to the Earth surface processes at a magnitude equivalent to such global stratigraphic events? For example, have humans impacted the delivery of sediment to the coastal ocean at a level equivalent to the magnitude of changes between the Pleistocene and the Holocene?

*Author for correspondence (james.syvitski@colorado.edu).

One contribution of 13 to a Theme Issue 'The Anthropocene: a new epoch of geological time?'.

The start of the Anthropocene depends on the eye of the beholder and the sub-discipline of science being considered. Based on surface-temperature records, the Anthropocene began in AD 1950 [3]. Other signals would locate the start of the Anthropocene earlier [3]: 1870 for accelerated sea-level rise and 1750 for increases in global atmospheric concentrations of CO_2, CH_4 and N_2O. Ruddiman [4] argues that the human footprint began with the spread of civilization and its introduction of agriculture, and the indirect consequences of land-use change for agriculture, *ca* 6000 years ago. We also know that human population increased by one order of magnitude, between 1600 and 1976, with their concomitant need for minerals, soil and aggregate, agriculture, energy, water, transportation and other infrastructure.

Nir [5] notes four factors that affect the intensity, volume and rate of human intervention in the environment—demography, history, economics and socioeconomics. Humans have (after [5] with modifications):

— intervened against the force of gravity,
— decelerated and accelerated natural processes,
— focused energy, and
— altered or destroyed ecosystems.

We can further add that humans have [3]:

— altered the Earth's atmospheric and ocean climatology and chemistry, extent of snow cover and permafrost, sea-ice extent, glacier and ice-sheet extent, sea level and indeed the hydrological cycle.

The focus of this paper is on Anthropocene-affected sediment fluxes. The impact of humans on sediment flux at a significant scale began some 3000 years ago within the Yellow River basin [6], but many polar rivers remain in near-pristine condition [7].

Known geomorphic activities involving humans include:

— deforestation and its associated role in soil erosion, slope failure and downstream sedimentation,
— farm-animal grazing leading to gully development and soil erosion,
— agriculture, including tillage, terracing, irrigation systems and subsurface water extraction, leading, respectively, to increased soil erosion, creep, siltation and subsidence,
— mining and its associated role in river channel and hill slope alteration, slope instabilities and subsidence,
— transportation systems, including gully development, soil erosion and riverbed scouring,
— waterway re-plumbing, including reservoirs and dams, diversions, channel levees, channel deepening, discharge focusing and ultimately coastline erosion,
— coastal management through groynes, jetties, seawalls, breakwaters and harbours, leading to unnatural coastal erosion or sedimentation, wetland, mangrove and dune alterations,
— warfare that magnifies many of the above activities for a duration that extends beyond the period of combat, and

— global climate warming and its impact on coastal inundation, precipitation intensity, including the intensity of cyclones, desertification and an accelerated hydrological cycle.

This paper reviews data and models useful in defining the timing and magnitude of human-influenced sediment flux, to better constrain the Anthropocene. The story is complex since human impacts on Earth surface processes are not spatially or temporally homogeneous. The paper provides examples on how direct human alteration may have secondary consequences on the future geological record—through floodplain and delta-plain function, sediment dispersal into the coastal ocean and seafloor resuspension by trawling.

2. Supply and flux of sediment along hydrological pathways

Sediment discharge responds both to the impact of humans and to changes in climate. Importantly, there is a time-dependent response to these impacts. For example, some fluvial systems are still responding as a delayed reaction to the former Pleistocene conditions. Ice sheets removed the soil cover of higher latitude regions, reorganized continental drainage patterns, left large regional areas covered with thousands of lakes and marshes, and mantled continental-scale tracts of land with ice-sheet deposits (till, eskers, drumlins, moraines). Long after the major ice-sheets melted, rivers were adjusting to climate-driven discharges in difference to melt-driven discharges [8]. This episode of adjustment by rivers reworking the Pleistocene sediment cover is known as a paraglacial response [9]. Ice-edge rivers such as the Ohio, Mississippi and Missouri, are still adjusting to this Pleistocene imprint [10] (for a full discussion, see [11]). In other parts of the world, rivers adjusted to new Holocene climate conditions, sometimes in response to a reorganization of jet-stream location and strength [12], or monsoon strength and direction [13]. This cautionary note warns us not to assign causality simply owing to coherency.

Humans have both increased the erosion of the landscape and intercepted the sediment along the hydrological pathways, sometimes simultaneously, sometimes in sequence. The major means for increasing a river's sediment load is through mining (e.g. Kolyma River [14]), deforestation (e.g. Dnestr River [14]; Amazon River [15]), conversion of pastureland to cropland (e.g. Magdalena River [16]), poor farming practices (e.g. Yellow River [6]) and through road construction (e.g. Lanyang River [17]). Land use is the dominant control on particulate fluxes in areas of low relief and large-scale urbanization [18]. Land clearing in low-relief areas may increase sediment yields by more than an order of magnitude [19]. Approximately 75 per cent of the elevated sediment yields of Mediterranean headwater basins are attributed to human activity [20].

Terracing of hillslopes and mountainsides for agricultural use is certainly one of the largest geomorphic processes for Asia including Indonesia. During the construction phase, terracing is a net producer of sediment into waterways, particularly since modern terracing involves heavy machinery, in contrast to the Mayan or early Chinese terracing methods. Once completed, terrace farming reduces the sediment flux into waterways, and remains an accepted form of soil

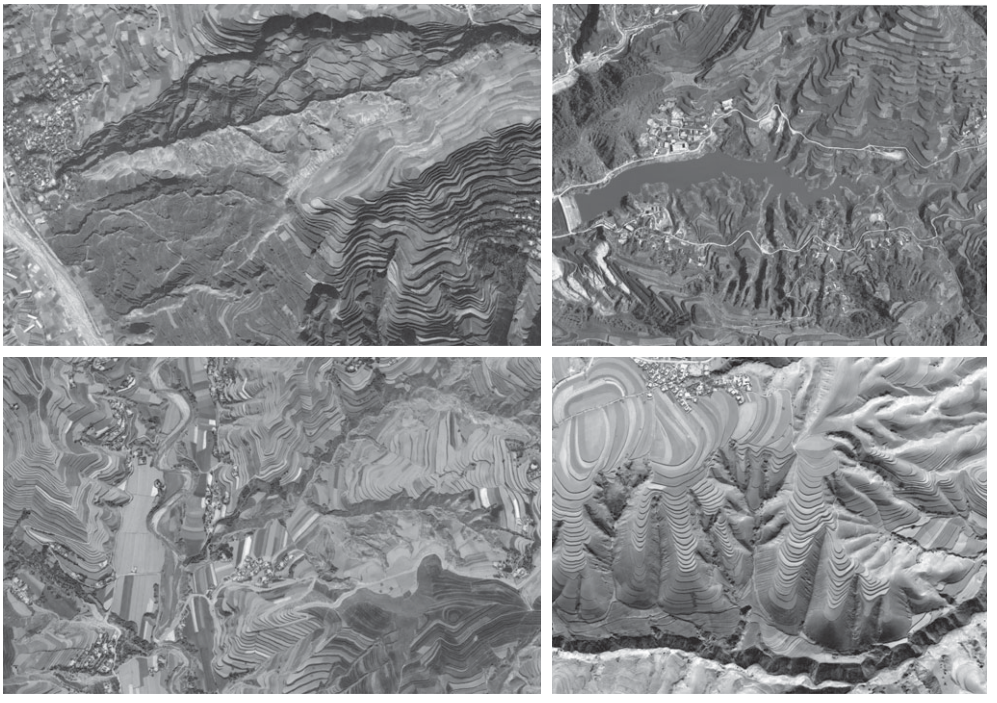

Figure 1. QuickBird satellite images from Digital Globe showing hillslope terracing in the Loess Plateau region, Yellow River, China. Each image represents 4–6 km in width; individual buildings provide a scale reference.

conservation. The sheer volume of mountain sculpturing however is so impressive (figure 1) that it probably produces a regional sediment flux signal at par with deforestation or reforestation.

Human activities may also compound a climate event with catastrophic consequences. A proliferation of small farms employing poor tilling practice on top of a prolonged drought in the central USA (Great Plains area) in the early 1930s led to one of the world's largest erosion events [21]. By 1938, the US Department of Agriculture tallied the loss of topsoil for $95\,100\,\mathrm{km}^2$ at 12.5 Gt ($1\,\mathrm{Gt} = 10^{12}\,\mathrm{kg}$). The sediment was dispersed widely into waterways, and even outside of the drainage basins to areas of New England.

The annual mass of sediment relocated by direct human intervention is likely to be at the scale of the fluvial sediment load delivered to the global coastal ocean, or approximately $15 \pm 0.5\,\mathrm{Gt\ yr}^{-1}$ [22], based on the upscaling of individual engineering projects for which we have good data. Four examples are described here. The first example is the Hull-Rust-Mahoning Mine in Hibbing, Minnesota, the largest open pit iron mine in the world (figure 2). Over 1.2 Gt of waste material and iron ore have been removed from the mine area, as ore shipments began in 1895.

The second example involves the Athabaska oil sand deposits in northern Canada, of which $14\,000\,\mathrm{km}^2$ is suitable for surface mining. The oil sands are typically 40–60 m thick and covered by less than 75 m of overburden (≤ 3 m of

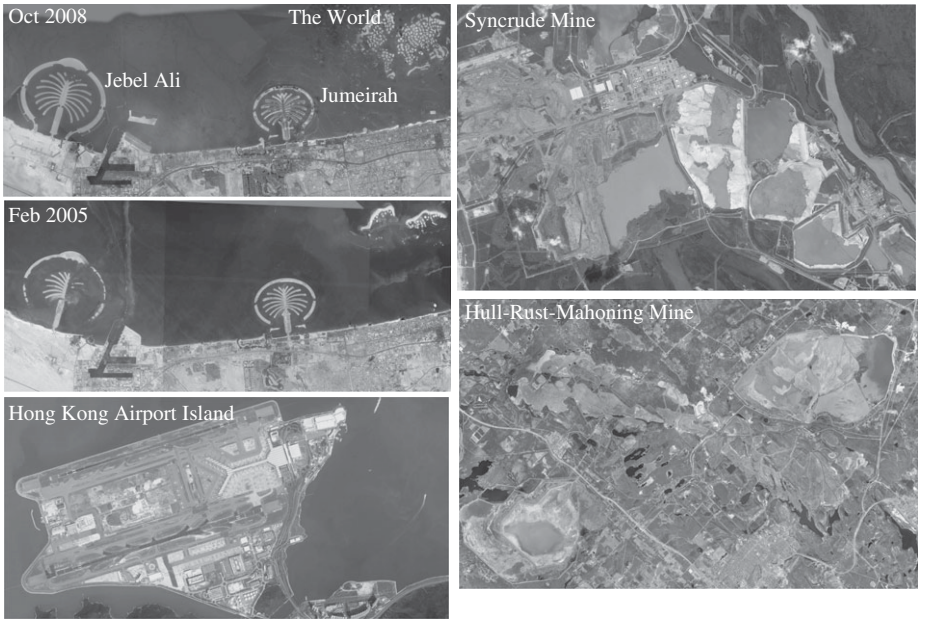

Figure 2. Four of the world's largest construction or mining sites (see text for details). Quickbird satellite images are from Digital Globe. The Palm Island images are 40 km in width; the Hong Kong Airport image is 7 km in width; the Syncrude Mine image is 15 km in width; and the Hull-Rust-Mahoning Mine is 22 km in width.

surface muskeg, ≤ 75 m of clay and barren sand). The Syncrude Mine, one of many mines in the area, is the largest at 191 km^2, with operations having already removed and processed 30 Gt of sediment (figure 2).

The third example is the Palm Islands construction, which will add 520 km of beaches to the city of Dubai, United Arab Emirates. Palm Jumeirah Island was created using 0.2 Gt of sand and rock poured onto the 10.5 m deep seabed (figure 2). Palm Jebel Ali island was created using 0.4 Gt of rock, sand and limestone (figure 2). Palm Deira island, when completed, will have used 2.0 Gt of sand. 'The World' will consume 0.55 Gt of sand and rock to create an artificial archipelago of various small islands constructed in the rough shape of a map of the landmasses of the Earth (figure 2).

The fourth example is the construction of the 12.5 km^2 Hong Kong Airport (figure 2), which involved dredging 108 Mm^3 marine clay, 76 Mm^3 of marine sand and a total volume of fill 197 Mm^3 [23]. Over 0.6 Gt of sediment was displaced. (How large is 0.6 Gt? The Great Wall of China is approx. $6\,250\,000 \times 7 \times 5$ m or approx. 0.4 Gt of Earth and stone.)

The major means to reduce the delivery of river sediment to the coast is through sediment retention in reservoirs [24]. Large reservoirs on average offer trapping efficiencies of 80 per cent [25]. Globally, there are more than 48 000 large dams (heights greater than 15 m, average height 31 m, average reservoir area 23 km^2), with more than 2000 large dams under construction. Most dams have been constructed since the 1940s (see figure 3 for growth in the USA). Prior to 1950, there were eight dams in China: by 1982 there were 18 600 dams or 55 per cent of the world total.

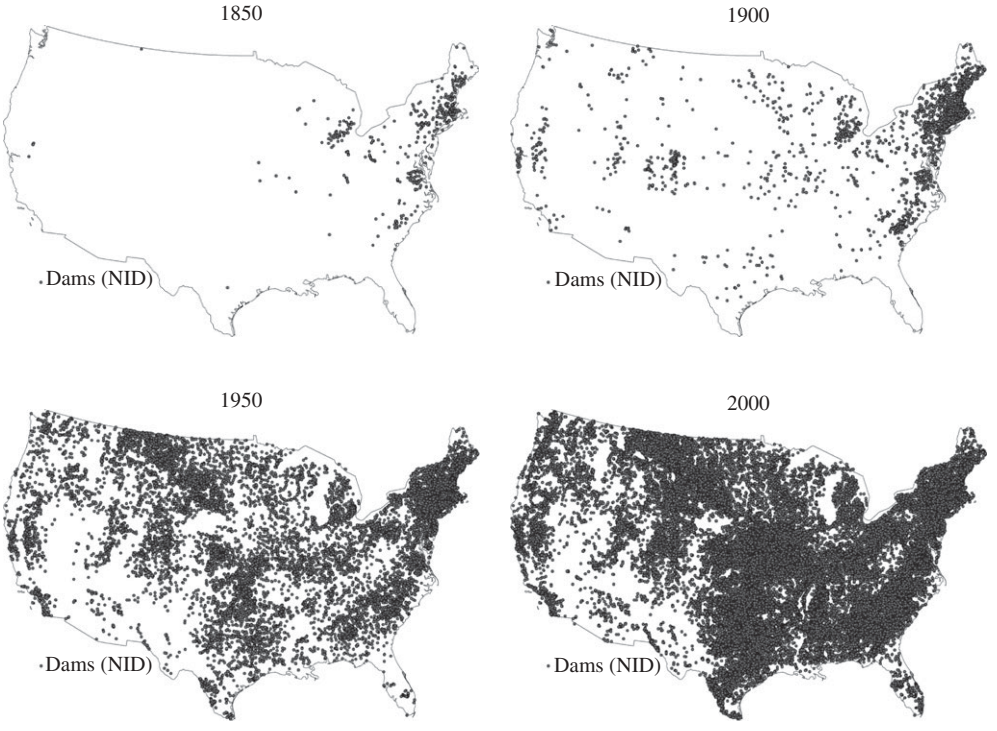

Figure 3. The growth of US dams and reservoirs as recorded in the National Inventory of Dams (NID). Four periods shown: 1850, 1900, 1950 and 2000. There were no dams in 1800.

Each reservoir affects the conveyance of sediment to the coastal zone to some degree. In contrast to early dams that were placed in highlands for the generation of hydroelectricity, reservoirs are increasingly placed within floodplains (figure 4) for flood control, recreation and for water diversion to meet irrigation needs [25]. Type examples of the impact of dams include the Nile and Colorado [26], Yenisey [27], Ebro [28], Danube [29] and Sao Francisco [30]. River diversions into agricultural canals also offer an effective way to reduce a river's sediment load (e.g. Indus River [31]), as does the hardening of riverbanks by raft and concrete [32].

The long-term (>30 years) suspended-sediment load of a river depends on [25]: (i) the geomorphic/geological influences of basin area, lithology and relief, (ii) geographical influences of basin temperature, runoff and ice extent, and (iii) human activities that may accelerate or mitigate soil erosion and/or trap sediment. The BQART model inherently incorporates the scaling of sediment production (chemical, mechanical and human erosion), sediment storage (lakes, reservoirs, floodplains) and flood-wave dynamics,

$$Q_{\mathrm{s}} = w[(1 - T_{\mathrm{E}})E_{\mathrm{h}}]ILQ^{0.31}A^{0.5}RT, \quad \text{for } T \geq 2^{\circ}\mathrm{C}, \tag{2.1}$$

and

$$Q_{\mathrm{s}} = 2w[(1 - T_{\mathrm{E}})E_{\mathrm{h}}]ILQ^{0.31}A^{0.5}R, \quad \text{for } T < 2^{\circ}\mathrm{C}, \tag{2.2}$$

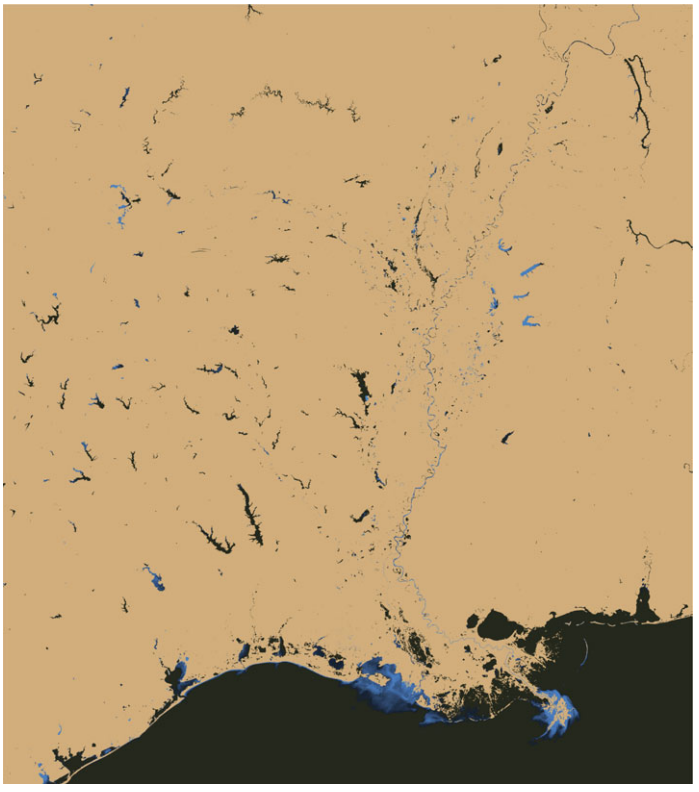

Figure 4. Water bodies in south central USA, with the Mississippi River and Delta as the viewer's frame of reference. Except for coastal lagoons enclosed by barrier islands and spits, most of the water bodies are man-made reservoirs. This enhanced satellite (Moderate Resolution Imaging Spectroradiometer Terra) image taken on 15 January 2002 is processed from near-infrared wavelengths. Black is clean water; blue defines water with high suspended-sediment concentration.

where $w = 0.02$ in units of $\mathrm{kg\,s^{-1}}$, or $w = 0.0006$ in units of $\mathrm{Mt\,yr^{-1}}$ ($1\,\mathrm{Mt} = 10^9\,\mathrm{kg}$), Q is the discharge of water in $\mathrm{km^3\ yr^{-1}}$, A is the drainage area in $\mathrm{km^2}$, R is the relief in km, T is the basin-averaged temperature in °C, I is the glacier erosion factor, L is the basin-averaged lithology factor, T_{E} is the trapping efficiency of lakes and reservoirs and E_{h} is the human-influenced soil-erosion factor (for details, see appendix A and [25]). The BQART formula provides a value on average within 38 per cent of the measured loads on 488 global rivers that drain 63 per cent of the global land surface. BQART is particularly aimed at capturing the wash load, as the observations were mostly from gauging stations near river mouths. The formula has since been shown to be successful in predicting the within-basin suspended load [33]. Rivers also deliver a coarser load in contact with the channel bed, known as bedload, which ranges from less than 1 to 20 per cent of the total sediment load for locations near river mouths, with a global average of 6.6 per cent [34].

Applying BQART using modern climatology and no human influences (appendix A), the pre-human suspended-sediment load or discharge to the coastal ocean is calculated as $15.1 \pm 0.5\,\mathrm{Gt\,yr^{-1}}$ (table 1). To calculate this sediment

Table 1. Flux of river water (Q) and sediment (Q_s) for pre-Anthropocene and Anthropocene conditions *ca* late twentieth century (after [35]). These values represent continental coastline fluxes.

continent	Q (km^3 yr^{-1})	Q_s with humans[a] (Gt yr^{-1})	Q_s pre-humans[a] (Gt yr^{-1})
Africa	3797	1.1	1.6
Asia	9806	4.8	5.3
Australasia	608	0.28	0.24
Europe	2680	0.4	0.6
Indonesia	4251	2.4	2.4
North America	5819	1.5	1.7
Oceans	20	0.004	0.003
South America	11 529	2.4	3.3
Global	38 510	12.8	15.1

[a]Incorrect Q_s values were unfortunately published in a previous table [35].

discharge as affected by humans, two datasets are merged: (i) observations (1960–1990) for 160 global rivers whose drainage basins collectively cover 60 per cent of the terrestrial land surface and (ii) BQART estimates for the remaining drainage basins using modern climatology, population density (PD), gross national product (GNP) per capita and reservoir characteristics (appendix A). The twentieth century global sediment load is calculated to be 12.8 ± 0.5 Gt yr^{-1}, a 15 per cent reduction in the amount of sediment delivered to the coastal zone (table 1). At the continental scale, the change between the Anthropocene and the pre-Anthropocene loads can vary more widely, reflecting different stages of industrial development [22], and by an order of magnitude for individual river basins [30].

Unfortunately, we have modest information on the historical variation in the sediment load of rivers: across centuries for a few rivers, and across four to five decades for perhaps another 100 rivers [25]. Except for Indonesia, parts of South America and polar regions not impacted by dams, the delivery of sediment to the coastal ocean has been decreasing globally (figure 5). Some rivers show loads increasing during the twentieth century (e.g. deforestation—Dnestr, Amazon; mining—Kolyma). Others such as the Yellow [6], Po [36] and Mississippi [37] had early increases in their sediment loads owing to human impact, but have since strongly decreased owing to the proliferation of dams and diversions within their drainage basins. This pattern is similar to the eastern seaboard of the USA [38], where pre-European settlement (pre-1740) saw sedimentation rates in estuaries increase eight times through early deforestation and agriculture (1750–1820), increase another three times during the period of peak deforestation and intensive agriculture (1820–1920) and finally reduce 10 times during the period of dam building and urbanization (1920 to present).

Most rivers (e.g. Danube, Yenisey) are carrying much less sediment [22], and some rivers transport virtually no sediment: Nile, Colorado, Ebro, Sao Francisco and Indus (figure 5). Sediment interception by reservoirs has reduced the global sediment delivery to the coast by about 10 years of pre-dam sediment transport. This reduced load represents a coastal volume of about 73 km^3, equivalent to an area of 7300 km^2 assuming a 10 m thick prograding wedge.

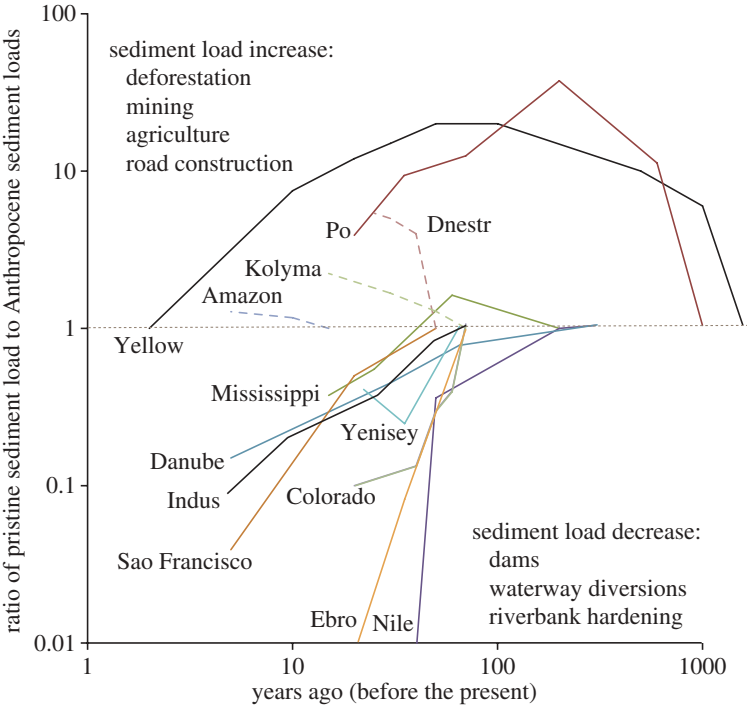

Figure 5. Relative changes in the sediment loads carried by select rivers. Note that climate variability has been removed from these trends, by taking averages across 10–20 years.

3. Floodplain and delta-plain function

Humans have worked to harness the world's freshwater resources for improved use (agriculture, industry, consumption, transportation), and for natural flood-hazard reduction. River pathways were thus fixed in location with stop-banks and levees. Some rivers are free to meander between these stop-banks within widths 10–100 times narrower than the natural floodplain widths. Other rivers even have their meanders fixed in space with hardened channel banks.

As a representative example, the Yellow River during the Late Holocene changed its route to the sea every few decades to centuries, across its 700 km wide floodplain (figure 6*a*). Extensive flooding and the deposition of cover deposits accompanied channel switching, until a new route was notched into the floodplain. Loss of life and infrastructure forced fifteenth to nineteenth century Chinese engineers to spatially fix the Yellow river within artificial levees, during the time when soil erosion of the Loess Plateau was near its maximum [6]. As a result of sediment aggradation within the levees, the river eventually became super-elevated 5–15 m above its floodplain (figure 6*b*,*c*). When the levees failed, a crevasse splay grew until the levee was repaired. A large levee failure in 1855 led to the establishment of a new course of the Yellow, after which and for 100 years the river transported enormous sediment loads (discharges of 1800 Mt yr^{-1} in the 1950s). The load has since been reduced to less than 200 Mt yr^{-1} owing to reservoir interception, soil conservation (figure 1), decreasing runoff and other

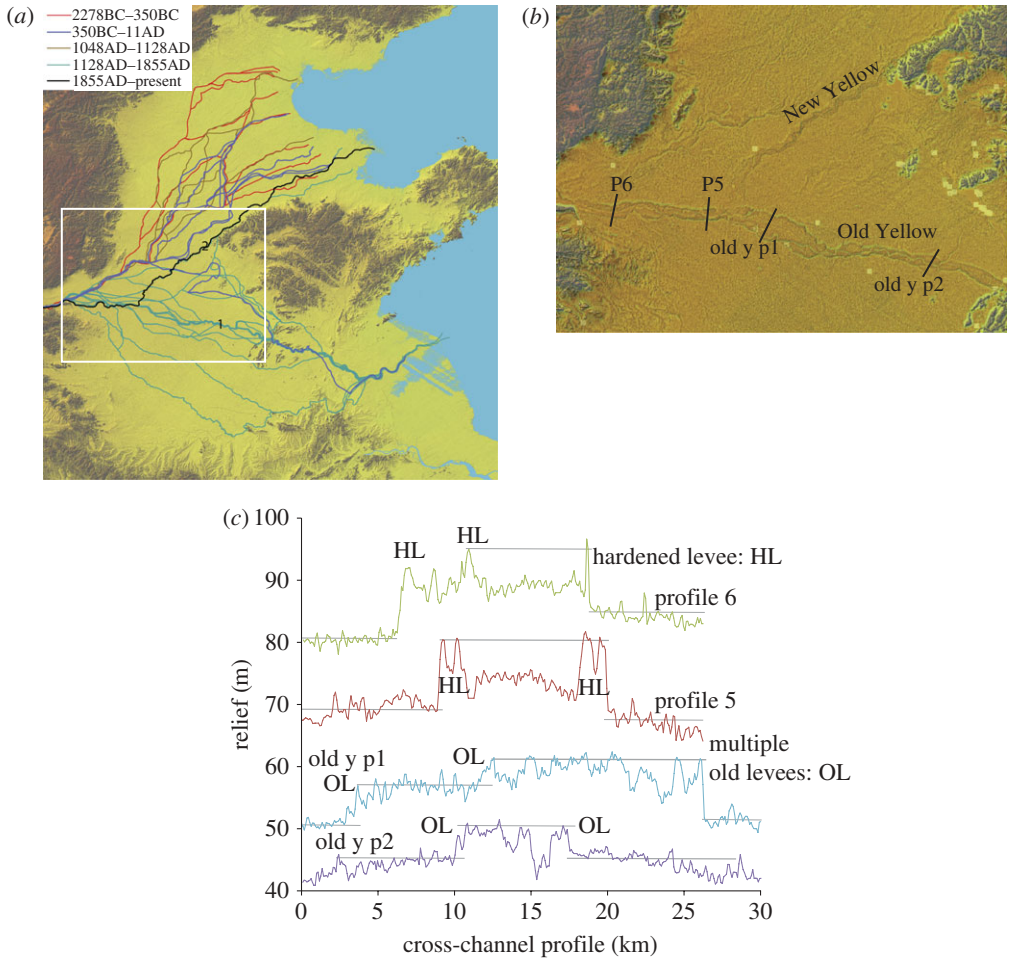

Figure 6. Yellow River (Huanghe) floodplain. (*a*) Yellow River historical paths superimposed on Shuttle Radar Topography Mission (SRTM) topographical data. Channel 1 is the main route between AD 1128 and AD 1855. Channel 2 is the path since 1855. (*b*) Expanded view of the junction between these old and new paths with sectional profiles indicated. SRTM data have been modified to accentuate low-level topography. (*c*) Sectional elevation profiles showing the super-elevation of the modern and palaeo channels and their levees.

human interventions [6,39]. The result is a new 15–30 m super-elevated river course across the floodplain, and the formation of a new delta in the Sea of Bohai (figure 6).

The post-1855 Yellow delta is one of a number of global deltas (e.g. Po, Ebro, Colorado in Texas) that have formed during the Early Anthropocene period of elevated sediment loads [34]. These same deltas and many others have entered a destructive phase, concomitant with the upstream sediment sequestration in reservoirs, and accelerated compaction. Controls on a delta's surface elevation are [30]

$$\Delta_{\mathrm{RSL}} = A - \Delta E - C_{\mathrm{n}} - C_{\mathrm{A}} \pm M, \tag{3.1}$$

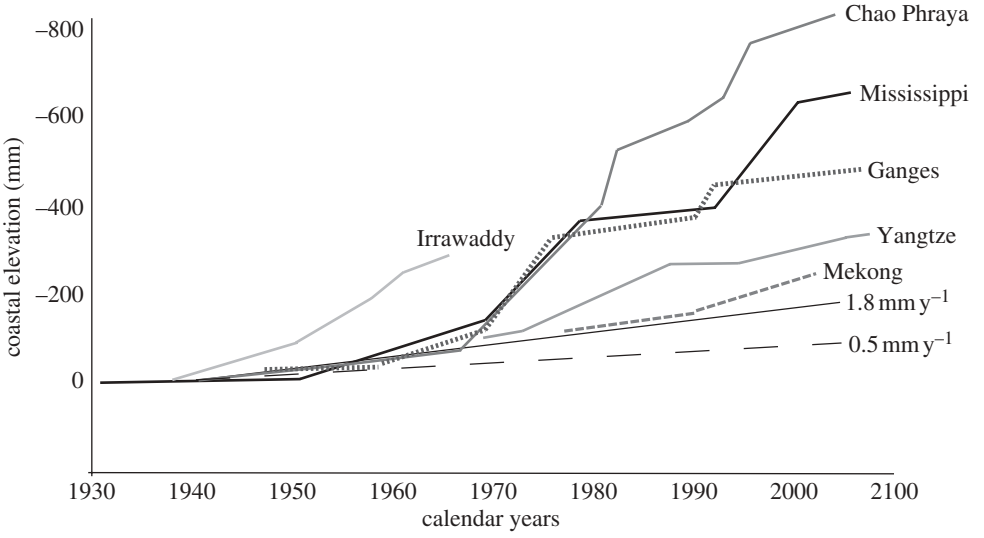

Figure 7. The relative rate of sea-level rise on selected deltas is many times faster than the ambient pre-Anthropocene sea-level rate of less than 0.5 mm yr^{-1} and the global warming eustatic sea-level rise of 1.8 mm yr^{-1}. Deltaic subsidence relates to natural and accelerated compaction, greatly reduced aggradation and the weight of the sediment load of the delta (isostasy).

where Δ_{RSL} is the vertical change in delta surface elevation, A is the sediment aggradation from sediment delivered to and retained on the subaerial delta surface as new sedimentary layers, ΔE is the eustatic sea-level rise owing to changes in the volume of the global ocean as influenced by the storage of terrestrial water in glaciers, ice sheets, groundwater, lakes and reservoirs, and from ocean temperature, C_n is the natural compaction from dewatering and grain-packing realignment and organic matter oxidation, C_A is the accelerated compaction as a consequence of subsurface oil, gas or groundwater mining, human-influenced soil drainage and accelerated oxidation, and M is the vertical movement of the land surface as influenced by the redistribution of Earth masses (e.g. sea-level fluctuations, growth of delta deposits, growth or shrinkage of nearby ice masses, tectonics and deep-seated thermal subsidence).

For many deltas, *aggradation rates* have either substantively decreased or nearly eliminated (e.g. Chao Phraya, Colorado, Nile, Po, Tone, Vistula, Yangtze and the Yellow River deltas). In addition to sediment sequestration in upstream reservoirs, the sediment flux across a delta plain is engineered through stop-banks to bypass the floodplain and directly enter the coastal ocean [30]. Deltas are also subsiding faster than in pre-Anthropocene times, as humans mine for groundwater and petroleum and thereby collapse their structure [40]. The Chao Phraya, Niger and Po are type examples [39]. Some deltas now suffer from virtually no aggradation and very high rates of accelerated compaction (e.g. Colorado, Nile, Pearl, Rhone, Sao Francisco, Tone, Yangtze and the Yellow). As a result, deltas are sinking many times faster than the rate of sea-level increase (figure 7).

Humans have also reduced the number of distributary channels that carry floodwaters across deltas, in aid of year-round shipping [30]. Fewer channels decrease the rate of delta-plain aggradation, locally increasing the rate of coastal-zone sedimentation near the remaining channel mouths, but also increasing the rate of coastal erosion in areas that once received distributary sediment flux [41]. The Indus and Nile are type examples of these Anthropocene phenomena [42].

4. Sediment dispersal by delta plumes

Distributary channels divide up the discharge from the main stem and thereby increase the hydraulic radius over which the river water flows [32]. Consequently, the velocity of effluent in a set of distributary channels is reduced relative to a main stem flow, along with its inertial ability to transport sediment away from the coast. With reduced momentum to power the seaward-flowing plumes emanating from these distributary mouths, more suspended sediment is trapped near these river mouth. As humans have reduced the number of distributary channels, greater dispersal of the fluvial-suspended load would occur. However, dam operations have reduced the magnitude of the seasonal flood wave [34] and consequently the dispersal of river sediment. If sediment retention on deltas is reduced (i.e. reduced aggradation rates), more sediment bypasses the delta and is delivered to the coastal ocean. From a coastal-ocean perspective, this may in fact make up for the lower conveyance of sediment to the delta owing to up-stream sequestration of sediment in reservoirs. Human influence on sediment dispersal is at the very least complex.

Most rivers deliver their sediment load through momentum-driven surface (hypopycnal) plumes given the strong density barrier to freshwater entering the coastal ocean. A river plume and its sedimentation depend on the discharge magnitude, the rate particles flocculate, the settling velocities of the flocs and the ambient currents and density structure including bottom boundary-layer dynamics. The critical concentration of suspended sediment needed to create a hyperpycnal plume in sea water is in the range of 35–45 $\mathrm{kg\,m^{-3}}$ [43] or perhaps larger [44]. Rivers that carry the requisite sediment concentration for hyperpycnal activity are typically small mountainous rivers that directly enter the ocean without an intervening floodplain. Hyperpycnal flows differ from surface plumes in that they hug the seafloor; bathymetry plays an important role in defining the flow path, along with ambient bottom currents as influenced by coastal upwelling or downwelling [45]. The bathymetry of shelves often offers a steeper gradient than the riverbed, and it is not uncommon for a hyperpycnal current to accelerate and become erosive as it plunges into the coastal ocean [46]. In contrast, surface plumes are more influenced by coastal winds, ambient surface currents, river momentum and buoyancy [47]. The offshore sedimentary record will differ depending on the dispersal mechanism of hypopycnal versus hyperpycnal plumes [48–50].

Humans have altered these mechanisms of sediment dispersal in contrasting ways:

— elevated suspended-sediment concentrations to such an extent that hyperpycnal currents are generated and
— reduced a river's sediment concentration so as to reduce or eliminate its ability to produce a hyperpycnal current.

The pre-Anthropocene sediment concentrations of the Yellow River, for example, would have been 5–10 times less than the twentieth century concentrations, assuming modern climatology. Thus, the pre-Anthropocene Yellow River would have generated only hypopycnal plumes [43]. In contrast, during 1950–1999, hyperpycnal events on the Yellow River occurred 33 d yr^{-1} on average and contributed approximately 52 per cent of the annual sediment delivery to the sea [51]. Since 2000 when new conservation practices were put in place, only the Yellow River generates hyperpycnal events 3 days each year (down from 33 days), accounting for approximately 24 per cent of the annual sediment load delivered to the sea [51].

The Waipaoa River, New Zealand, experienced an eightfold increase in its sediment load for the last 150 years over the pre-Anthropocene flux [52]. Specifically, the establishment of Polynesian settlements 600 years ago was associated with an increase in suspended-sediment discharge by 140 per cent, whereas the wholesale land-use changes effected by European colonists initially caused suspended-sediment discharge to increase by 350 per cent, and by 660 per cent once the headwaters were deforested [52]. Model simulations show that 25 per cent of the total sediment discharge of the Waipaoa into the coastal ocean is presently via short-lived hyperpycnal flows, a process that began in the 1880s [53]. Prior to that for the previous 3000 years, only four hyperpycnal floods occurred.

Other studies have shown the increased likelihood of Anthropocene hyperpycnal activity when, in more pristine times, a river was unlikely to generate hyperpycnal discharges (e.g. Eel River, USA [54]; Tet River, Spain [55]; Lanyang River, Taiwan [17]). In contrast to these situations, the Apennine Rivers of Italy have lost most of their capability of producing hyperpycnal flows owing to dam operations [36], as has the Tet River with the onset of dam operations [55].

5. Seafloor erosion through trawling

While the role of agricultural practices on soil erosion has been well studied, only recently has the role of resuspension by bottom trawling on continental shelves been investigated. Areas of strong fishing activity can modify the scale of natural disturbance by waves and currents [56]. The impact of bottom trawls on fine sediment resuspension per unit surface is comparable with that of the largest storms, and is responsible for more than 30 per cent of the total export of suspended sediment from the shelf of the Gulf of Lions [56]. Unfortunately, the global impact of seafloor trawling on the magnitude of sediment disturbance has not yet been made, but is expected to be large.

6. Summary

Major impacts by humans on soil erosion began 3000 years ago following growth in human population in a few river basins. Impacts accelerated more widely 1000 years ago. By the sixteenth century, soil disturbance was rampant as modern societies began engineering their environments. By the early twentieth century, mechanization related to Earth removal, mining, terracing and deforestation led to global signals in increased sediment discharge in most large rivers. By the 1950s, this sediment-discharge signal reversed for most major rivers owing to the

proliferation of dams. A trend of subsidence outstripping sedimentation began in the 1930s for some deltas and for many deltas has become a dominant signal in terms of relative sea-level, overwhelming even the global warming imprint on global sea level. These collective impacts have given rise to major changes on how water and sediment flows across continents and is subsequently discharged into the sea. Hyperpycnal flow events have become more common for some rivers, and less common for other rivers. The marine environment remains cloaked in mystery, being largely hidden from satellite surveying. Simplified calculations on the phenomena of trawling suggest that even continental shelves have received a significant Anthropocene impact.

It is this author's estimation then that the Anthropocene imprint on the landscape does rise to the level of a geological transition such as between the Pleistocene and the Holocene. Other studies support this sediment-flux magnitude-level comparison [57]. This Anthropocene signal deal is thus much broader than the recent global warming signal much discussed by governments. Further, because the human imprint on sediment flux to and through coastal environments is a developing story with complex scenarios, its impact remains under-appreciated.

The authors thank Irina Overeem for an initial version of figure 7. Discussions with John Milliman and Bob Meade have led to insights incorporated in this article. The authors thank the US National Science Foundation and the US National Atmospheric and Space Administration for supporting various aspect of the study (NSF for model efforts, NASA for remote-sensing efforts). This paper forms a contribution to the Land Ocean Interaction in the Coastal Zone IGBP project.

Appendix A. Global application of BQART

The BQART model of Syvitski & Milliman [58] for determining the long-term sediment load of a river is

$$Q_s = w[(1 - T_E)E_h]ILQ^{0.31}A^{0.5}RT, \quad \text{for } T \geq 2^\circ\text{C},$$

and

$$Q_s = 2w[(1 - T_E)E_h]ILQ^{0.31}A^{0.5}R, \quad \text{for } T < 2^\circ\text{C},$$

where $w = 0.02$ in units of kg s^{-1}, or $w = 0.0006$ in units of Mt yr^{-1}, Q is the discharge in km^3 yr^{-1}, A is the drainage area in km^2, R is the relief in km, T is the basin-averaged temperature in °C and I is the glacier erosion factor defined as $I = (1 + 0.09A_g)$, where A_g is the area of the drainage basin as a percent of the total drainage area. L is the basin-averaged lithology factor defined as: $L = 0.5$ for basins comprised principally of hard, acid plutonic and/or high-grade metamorphic rocks, $L = 0.75$ for basins of mostly hard lithologies, $L = 1.0$ for basins of volcanic or basaltic rocks, or carbonate outcrops, or mixtures of hard and soft lithologies, $L = 1.5$ for basins with softer lithologies but with some harder lithologies, $L = 2.0$ for basins of sedimentary rocks, unconsolidated sediment cover or alluvial deposits and $L \geq 3$ for basins with exceptionally weak rock or loess deposits. T_E is the trapping efficiency of lakes and reservoirs, such that $(1 - T_E) \leq 1$. E_h is the human-influenced soil-erosion factor based on PD and GNP per capita: $E_h = 0.3$ for basins with PD > 200 km^2 and GNP per capita greater than \$15 000 yr^{-1}, $E_h = 1$ for low human-footprint basins (PD < 50 km^2)

or those containing competing influences of soil erosion and conservation, $E_h = 2.0$ for basins where PD $> 200\,\mathrm{km}^2$ and GNP per capita is $\leq \$2500\,\mathrm{yr}^{-1}$ ($\$ =$ US dollar 2003). For details on the parameters, readers are referred to the original article [58].

To complete a global analysis of the sediment flux delivered to the world's coastal ocean, we obtained geo-referenced data layers for each of the BQART terms (equation (2.1)), at a minimum resolution of 30 min (latitude × longitude, approx. 60 000 grid cells). We next determined the integrated basin-wide parameter values for each of the 4464 river basins defined in the University of New Hampshire (UNH) Simulated Topological Network (STN-30p) for potential river flow paths [59]. These basins do not include the drainage basins covered by the ice sheets of Antarctica, Greenland and portions of the Canadian Archipelago, or those that do not have a positive discharge to the coastal ocean or sea (see [59] for details). Our data layers include the following:

— PD from 2000 (based on United Nations Educational, Scientific and Cultural Organization (UNESCO) data; http://wwdrii.sr.unh.edu/download.html),
— Gross National Income per capita (GNI) from 2005, formerly GNP (World Bank; http://www.worldbank.org/),
— lithology using a re-integration of the Dürr *et al.* [60] digital lithology map onto STN-30p drainage basins [35],
— basin surface temperatures calculated from National Centers for Environmental Prediction (NCEP)/National Center for Atmospheric Research (NCAR) reanalysis data from the National Oceanic and Atmospheric Administration (NOAA)-Cooperative Institute for Research in Environmental Sciences (CIRES) Climate Diagnostic Center, averaged across 30 years [61],
— relief obtained from the Global 30 Arc-Second Elevation Dataset (GTOPO-30) global digital-elevation model established in 1996 (http://edc.usgs.gov/products/elevation/gtopo30/gtopo30.html),
— catchment areas using STN-30p have a 7.5 per cent absolute error, and a 2 per cent bias,
— ice cover from the National Snow and Ice Data Center [62],
— composite discharge field comes from monthly values (1970–1999) derived from the Global Runoff Data Centre (GRDC) covering 72 per cent of the world's actively discharging landmass, merged with simulations based on modern climatology using the UNH Water Balance and Transport Model (WBM/WTM) to provide discharge values where observations are not available (see [59] for details), and
— reservoir trapping embedded into the UNH WBM/WTM [59,63].

To arrive at the pre-human flux of sediment, we used the modern climatology (basin-averaged temperature and discharge), we set E_h in equation (2.1) equal to 1 and assumed there were no artificial reservoirs. The pre-human flux (table 1) was adjusted for the world's two largest rivers, the Amazon and the Congo, by adjusting their values to modern values—it is recognized that BQART over-predicts the sediment delivery on giant tropical rivers. There are competing hypothesis for this over-prediction by BQART. Firstly, the impact of a few high mountains may be over-emphasized, given the gigantic size of

their catchments (e.g. Congo River). Secondly, giant rivers often have significant intra-montane basins and foreland basin fans and floodplains that trap much of the seaward transiting sediment (e.g. Amazon River). Thirdly, Equatorial jungles may give up much less sediment on exceedingly flat floodplains, compared with more temperate basins. Testing these competing hypotheses is an active field of research.

References

1 Crutzen, P. J. & Stoermer, E. F. 2000 The 'Anthropocene'. *Glob. Change Newsl.* **41**, 17–18.
2 Zalasiewicz, J. *et al.* 2008 Are we now living in the Anthropocene? *GSA Today* **18**, 4–8. (doi:10.1130/GSAT01802A.1)
3 International Panel on Climate Change (IPCC) 2007 Climate change 2007: synthesis report. In *Contribution of Working Groups I, II and III to the Fourth Assessment Report of the Intergovernmental Panel on Climate Change* (eds Core Writing Team, R. K. Pachauri & A. Reisinger), pp. 104. Geneva, Switzerland: IPCC.
4 Ruddiman, W. F. 2003 The Anthropogenic greenhouse era began thousands of years ago. *Clim. Change* **61**, 261–293. (doi:10.1023/B:CLIM.0000004577.17928.fa)
5 Nir, D. 1983 *Man, a geomorphological agent: an introduction to anthropic geomorphology.* Jerusalem, Israel: Keter Publication Jerusalem.
6 Wang, H., Yang, Z., Saito, Y., Liu, J. P. & Sun, X. 2007 Stepwise decreases of the Huanghe (Yellow River) sediment load (1950–2004): impacts from climate changes and human activities. *Glob. Planet. Change* **57**, 331–354. (doi:10.1016/j.gloplacha.2007.01.003)
7 Syvitski, J. P. M. 2003 Supply and flux of sediment along hydrological pathways: research for the 21st century. *Glob. Planet. Change* **39**, 1–11. (doi:10.1016/S0921-8181(03)00008-0)
8 Kettner, A. J. & Syvitski, J. P. M. 2008 Predicting discharge and sediment flux of the Po River, Italy since the Late Glacial Maximum. In *Analogue and numerical forward modelling of sedimentary systems: from understanding to prediction*, vol. 40 (eds P. L. de Boer, G. Postma, C. J. van der Zwan, P. M. Burgess & P. Kukla), pp. 171–189. Oxford, UK: Special Publication of the International Association of Sedimentology.
9 Forbes, D. & Syvitski, J. P. M. 1995 Paraglacial coasts. In *Coastal evolution* (eds C. Woodruffe & R. W. G. Carter), pp. 373–424. Cambridge, UK: Cambridge University of Press.
10 Blum, M. D. & Törnqvist, T. E. 2000 Fluvial responses to climate and sea-level change: a review and look forward. *Sedimentology* **47**, 2–48. (doi:10.1046/j.1365-3091.2000.00008.x)
11 Sidorchuk, A. 2003 Floodplain sedimentation: inherited memories. *Glob. Planet. Change* **39**, 13–30. (doi:10.1016/S0921-8181(03)00011-0)
12 Morehead, M., Syvitski, J. P. & Hutton, E. W. H. 2001 The link between abrupt climate change and basin stratigraphy: a numerical approach. *Glob. Planet. Sci.* **28**, 107–127. (doi:10.1016/S0921-8181(00)00068-0)
13 Goodbred Jr, S. L. & Kuehl, S. A. 2000 Enormous Ganges–Brahmaputra sediment load during strengthened Early Holocene monsoon. *Geology* **28**, 1083–1086. (doi:10.1130/0091-7613(2000)28<1083:EGSDDS>2.0.CO;2)
14 Walling, D. E. & Fang, D. 2003 Recent trends in the suspended sediment loads of the world's rivers. *Glob. Planet. Change* **39**, 111–126. (doi:10.1016/S0921-8181(03)00020-1)
15 Martinez, J. M., Guyot, J. L., Filizola, N. & Sondag, F. 2009 Increase in suspended sediment discharge of the Amazon River assessed by monitoring network and satellite data. *Catena* **79**, 257–264. (doi:10.1016/j.catena.2009.05.011)
16 Restrepo, J. D. & Syvitski, J. P. M. 2006 Assessing the effect of natural controls and land use change on sediment yield in a major Andean river: the Magdalena drainage basin, Colombia. *Ambio* **35**, 65–74. (doi:10.1579/0044-7447(2006)35[65:ATEONC]2.0.CO;2)
17 Syvitski, J. P. M., Kettner, A., Peckham, S. D. & Kao, S. J. 2005 Predicting the flux of sediment to the coastal zone: application to the Lanyang watershed, northern Taiwan. *J. Coast. Res.* **21**, 580–587. (doi:10.2112/04-702A.1)

18 Wasson, R. J. 1996 Land use and climate impacts on fluvial systems during the period of agriculture. PAGES workshop report, series 96-2. See http://www.pages-igbp.org/products/pages_reports/fluvial.pdf.
19 Douglas, I. 1993 Sediment transfer and siltation. In *The earth as transformed by human action* (eds B. L. Turner, W. C. Clark, R. W. Kates, J. F. Richards, J. T. Mathews & W. B. Meyer), pp. 215–234. Cambridge, UK: Cambridge University Press.
20 Dedkov, A. P. & Mozzherin, V. I. 1992 Erosion and sediment yield in mountain regions of the world. In *Erosion, debris flows and environment in mountain regions*, vol. 209 (eds D. E. Walling, T. R. Davies & B. Hasholt), pp. 29–36. Wallingford, UK: International Association of Hydrological Sciences (IAHS) Publication.
21 Johnson, V. 1947 *Heaven's tableland: the dust bowl story.* New York, NY: Farrar, Straus, and Co.
22 Syvitski, J. P. M., Vörösmarty, C., Kettner, A. J. & Green, P. 2005 Impact of humans on the flux of terrestrial sediment to the global coastal ocean. *Science* **308**, 376–380. (doi:10.1126/science.1109454)
23 Syvitski, J. P. M., Harvey, N., Wollanski, E., Burnett, W. C., Perillo, G. M. E. & Gornitz, V. 2005 Dynamics of the coastal zone. In *Global fluxes in the Anthropocene* (eds C. J. Crossland, H. H. Kremer, H. J. Lindeboom, J. I. Marshall Crossland & M. D. A. Le Tissier), pp. 39–94. Berlin, Germany: Springer. (doi:10.1007/3-540-27851-6_2)
24 Vörösmarty, C., Meybeck, M., Fekete, B., Sharma, K., Green, P. & Syvitski, J. P. M. 2003 Anthropogenic sediment retention: major global-scale impact from the population of registered impoundments. *Glob. Planet. Change* **39**, 169–190. (doi:10.1016/S0921-8181(03)00023-7)
25 Syvitski, J. P. M. & Milliman, J. D. 2007 Geology, geography and humans battle for dominance over the delivery of sediment to the coastal ocean. *J. Geol.* **115**, 1–19. (doi:10.1086/509246)
26 Milliman, J. D. & Syvitski, J. P. M. 1992 Geomorphic/tectonic control of sediment discharge to the ocean: the importance of small mountainous rivers. *J. Geol.* **100**, 525–544. (doi:10.1086/629606)
27 Bobrovitskaya, N. M., Zubkova, C. & Meade, R. H. 1996 Discharges and yields of suspended sediment in the Ob' and Yenisey Rivers of Siberia. In *Erosion and sediment yield: global and regional perspectives* (eds D. E. Walling & B. W. Webb), pp. 115–123. Wallingford, UK: IAHS Publication 236, IAHS Press.
28 Liquete, C., Canals, M., Arnau, P., Urgeles, R. & Durrieu de Madron, X. 2004 The impact of humans on strata formation along Mediterranean margins. *Oceanography* **17**, 70–79.
29 Giosan, L., Bokuniewicz, H. J., Panin, N. & Postolache, I. 1999 Longshore sediment transport pattern along the Romanian Danube delta coast. *J. Coast. Res.* **15**, 859–871.
30 Syvitski, J. P. M. *et al.* 2009 Sinking deltas. *Nat. Geosci.* **2**, 681–689. (doi:10.1038/ngeo629)
31 Giosan, L. Constantinescu, S., Clift, P. D., Tabrez, A. R., Danish, M. & Inam, A. 2006 Recent morphodynamics of the Indus delta shore and shelf. *Cont. Shelf Res.* **26**, 1668–1684. (doi:10.1016/j.csr.2006.05.009)
32 Syvitski, J. P. M., Kettner, A. J., Correggiari, A. & Nelson, B. W. 2005 Distributary channels and their impact on sediment dispersal. *Mar. Geol.* **222–223**, 75–94. (doi:10.1016/j.margeo.2005.06.030)
33 Kettner, A. J., Restrepo, J. D. & Syvitski, J. P. M. 2010 A spatial simulation of fluvial sediment fluxes within an Andean drainage basin, the Magdalena River, Colombia. *J. Geol.* **118**, 363–379. (doi:10.1086/652659)
34 Syvitski, J. P. M. & Saito, Y. 2007 Morphodynamics of deltas under the influence of humans. *Glob. Planet. Changes* **57**, 261–282. (doi:10.1016/j.gloplacha.2006.12.001)
35 Syvitski, J. P. M. & Kettner, A. J. 2008 Scaling sediment flux across landscapes. In *Sediment dynamics in changing environments* (eds J. Schmidt, T. Cochrane, C. Phillips, S. Elliot, T. Davies, & L. Basher), pp. 149–156. International Association of Hydrological Sciences (IAHS) publication no. 325. Wallingford, UK: IAHS Press.
36 Syvitski, J. P. M. & Kettner, A. 2007 On the flux of water and sediment into the Northern Adriatic. *Cont. Shelf Res.* **27**, 296–308. (doi:10.1016/j.csr.2005.08.029)

37 Meade, R. H. 1996 River-sediment inputs to major deltas. In *Sea-level rise and coastal subsidence* (eds J. D. Milliman & B. U. Haq), pp. 63–65. Dordrecht, The Netherlands: Kluwer Academic Publishers.
38 Pasternak, G. B., Brush, G. S. & Hilgartner, W. B. 2001 Impact of historic land-use change on sediment delivery to a Chesapeake Bay subestuarine delta. *Earth Surf. Proc. Land.* **26**, 409–427. (doi:10.1002/esp.189)
39 Syvitski, J. P. M. 2008 Deltas at risk. *Sust. Sci.* **3**, 23–32. (doi:10.1007/s11625-008-0043-3)
40 Saito, Y., Chaimanee, N., Jarupongsakul, T. & Syvitski, J. P. M. 2007 Shrinking megadeltas in Asia: sea-level rise and sediment reduction impacts from case study of the Chao Phraya delta. *Inprint Newsletter of the IGBP/IHDP Land Ocean Interaction in the Coastal Zone* **2**, 3–9. See http://www.loicz.org/products/publication/newsletter/index.html.en.
41 Giosan, L., Constantinescu, S., Clift, P. D., Tabrez, A. R., Danish, M. & Inam, A. 2006 Recent morphodynamics of the Indus delta shore and shelf. *Cont. Shelf Res.* **26**, 1668–1684. (doi:10.1016/j.csr.2006.05.009)
42 Overeem, I. & Syvitski, J. P. M. 2009 Dynamics and vulnerability of delta systems. LOICZ reports and studies, no. 35, GKSS Research Center, Geesthacht, pp. 54.
43 Mulder, T. & Syvitski, J. P. M. 1995 Turbidity currents generated at river mouths during exceptional discharge to the world oceans. *J. Geol.* **103**, 285–298. (doi:10.1086/629747)
44 Lamb, M. P., McElroy, B., Kopriva, B., Shaw, J. & Mohrig, D. 2010 Linking river-flood dynamics to hyperpycnal-plume deposits: experiments, theory and geological implications. *Geol. Soc. Am. Bull.* **122**, 1389–1400. (doi:10.1130/B30125.1)
45 Imran, J. & Syvitski, J. P. M. 2000 Impact of extreme river events on the coastal ocean. *Oceanography* **13**, 85–92.
46 Khan S. M., Imran, J., Bradford, S. & Syvitski, J. P. M. 2005 Numerical modeling of hyperpycnal plume. *Mar. Geol.* **222–223**, 193–211. (doi:10.1016/j.margeo.2005.06.025)
47 Syvitski, J. P. M. *et al.* 2007 Prediction of margin stratigraphy. In *Continental-margin sedimentation: from sediment transport to sequence stratigraphy* (eds C. A. Nittrouer, J. A. Austin, M. E. Field, J. H. Kravitz, J. P. M. Syvitski & P. L. Wiberg), pp. 459–530. International Association of Sedimentologists Special Publication no. 37. Malden, MA: Blackwell.
48 Pratson, L. F., Hutton, E. W. H., Kettner, A. J., Syvitski, J. P. M., Hill, P. S., Douglas A. G. & Milligan, T. G. 2007 The impact of floods and storms on the acoustic reflectivity of the inner continental shelf: a modeling assessment. *Cont. Shelf Res.* **27**, 542–559. (doi:10.1016/j.csr.2005.12.018)
49 Wheatcroft, R. A. *et al.* 2007 Post-depositional alteration and preservation of sedimentary strata. In *Continental-margin sedimentation: from sediment transport to sequence stratigraphy* (eds C. A. Nittrouer, J. A. Austin, M. E. Field, J. H. Kravitz, J. P. M. Syvitski & P. L. Wiberg), pp. 101–155. International Association of Sedimentologists Special Publication no. 37. Malden, MA: Blackwell.
50 Kettner A. J., Gomez, B., Hutton, E. W. H. & Syvitski, J. P. M. 2008 Late Holocene dispersal and accumulation of terrigenous sediment on Poverty Shelf, New Zealand. *Basin Res.* **21**, 253–267. (doi:10.1111/j.1365-2117.2008.00376.x)
51 Wang, H., Bi, N., Saito, Y., Wang, Y., Sun, X., Zhang, J. & Yang, Z. 2010 Recent changes in sediment delivery by the Huanghe (Yellow River) to the sea: causes and environmental implications in its estuary. *J. Hydrol.* **391**, 302–313. (doi:10.1016/j.jhydrol.2010.07.030)
52 Kettner A. J., Gomez, B. & Syvitski, J. P. M. 2007 Modeling suspended sediment discharge from the Waipaoa River system, New Zealand: the last 3000 years. *Water Resour. Res.* **43**, W07411. (doi:10.1029/2006WR005570)
53 Hutton, E. W., Kettner, A. J., Kubo, Y., Gomez, B. & Syvitski, J. P. M. 2007 Simulating the effects of hyperpycnal events on the stratigraphy of Poverty Shelf, New Zealand. *Eos Trans. AGU* **88** (Fall Meet. Suppl., Abstract H41B-0503).
54 Morehead, M. D. & Syvitski, J. P. 1999 River Plume sedimentation modeling for sequence stratigraphy: application to the Eel Shelf, California. *Mar. Geol.* **154**, 29–41. (doi:10.1016/S0025-3227(98)00101-7)
55 Kettner, A. J. & Syvitski, J. P. M. 2009 Fluvial responses to environmental perturbations in the Northern Mediterranean since the Last Glacial Maximum. *Quat. Sci. Rev.* **28**, 2386–2397. (doi:10.1016/j.quascirev.2009.05.003)

56 Ferré, B., Durrieu de Madron, X., Estournel, C., Ulses, C. & Le Corre, G. 2008 Impact of natural (waves and currents) and anthropogenic (trawl) resuspension on the export of particulate matter to the open ocean: application to the Gulf of Lion (NW Mediterranean). *Cont. Shelf Res.* **28**, 2071–2091. (doi:10.1016/j.csr.2008.02.002)
57 Dearing, J. A. & Jones, R. T. 2003 Coupling temporal and spatial dimensions of global sediment flux through lake and marine sediment records. *Glob. Planet. Change* **39**, 147–168. (doi:10.1016/S0921-8181(03)00022-5)
58 Syvitski, J. P. M. & Milliman, J. D. 2007 Geology, geography and humans battle for dominance over the delivery of sediment to the coastal ocean. *J. Geol.* **115**, 1–19. (doi:10.1086/509246)
59 Syvitski, J. P. M., Vörösmarty, C., Kettner, A. J. & Green, P. 2005 Impact of humans on the flux of terrestrial sediment to the global coastal ocean. *Science* **308**, 376–380. (doi:10.1126/science.1109454)
60 Dürr, H. H., Meybeck, M. & Dürr, S. H. 2005 Lithologic composition of the Earth's continental surfaces derived from a new digital map emphasizing riverine material transfer. *Glob. Biogeochem. Cycles* **19**, GB4S10. (doi:10.1029/2005GB002515)
61 Syvitski, J. P. M., Peckham, S. D., Hilberman, R. D. & Mulder, T. 2003 Predicting the terrestrial flux of sediment to the global ocean: a planetary perspective. *Sediment. Geol.* **162**, 5–24. (Erratum *Sediment. Geol.* **164**, 345). (doi:10.1016/j.sedgeo.2003.11.001)
62 Armstrong, R., Raup, B., Khalsa, S. J. S., Barry, R., Kargel, J., Helm, C. & Kieffer, H. 2005 *GLIMS glacier database*. Boulder, CO: National Snow and Ice Data Center.
63 Vörösmarty, C., Meybeck, M., Fekete, B., Sharma, K., Green, P. & Syvitski, J. P. M. 2003 Anthropogenic sediment retention: major global-scale impact from the population of registered impoundments. *Glob. Planet. Change* **39**, 169–190. (doi:10.1016/S0921-8181(03)00023-7)